

# DFT Calculations of IR and Raman Spectra of Ru(bpy)<sub>2</sub>(CN)<sub>2</sub> Complex

B. Minaev, V. Minaeva, G. Baryshnikov\*, H. Agren\*\* and M. Girtu\*\*\*

\*Bogdan Khmel'nitskii National University, Cherkassy, Ukraine, [bmin@rambler.ru](mailto:bmin@rambler.ru)

\*\*The Royal Institute of Tehnology, Stockholm, Sweden, [agren@theochem.kth.se](mailto:agren@theochem.kth.se)

\*\*\*Ovidius University, Constanca, Romania, [girtu@univ-ovidius.ro](mailto:girtu@univ-ovidius.ro)

## ABSTRACT

Harvesting energy directly from sunlight using photovoltaic technology is an essential component of the future global energy production programs [1]. Photovoltaic devices, or solar cells, are based on the photoelectric effect, in which the incoming solar photons are absorbed in a sensitized semiconductor material freeing electric charges that are used to energize an external circuit [2]. The solar cells on the bases of nanocrystalline TiO<sub>2</sub> are usually sensitized by metal-organic dyes such as Ru-complexes with phenylpyridine and bipyridine ligands. The incident photon to current conversion efficiency (IPCC) in the wavelength region 400-600 nm can be rather high [1, 2]. In order to improve the IPCC value the heavier metal ions could be tested. Such sensitizers as coumarin, porphyrins, chlorophyll derivatives, antenna-sensitizer polynuclear complexes and eosin have been studied and reported to be less efficient than the most effective Ru-based sensitizing dyes, called the black dye (BD) and N3 dye [2-4], used for the nanocrystalline TiO<sub>2</sub> solar cell. In this paper we are planning to understand the IPCE of a new dye-sensitizer in order to predict the higher absorption efficiency to solar spectrum and higher electron transfer rate from redox systems to oxidized dye. Some simple Ru(II)(bpy)<sub>2</sub>(CN)<sub>2</sub> complex is studied by DFT method with optimized structure and vibrational analysis in order to predict the role of vibronic perturbations in spectra and interface electron transfer rate.

**Keywords:** solar cell, density functional, Ru-complexes, IR and Raman spectra.

## 1. METHOD OF CALCULATION

The density functional method (DFT) with the hybrid B3LYP functional and the Lan12DZ basis set [5-9] is used for geometry optimization of the Ru(II)(bpy)<sub>2</sub>(CN)<sub>2</sub> complex (Fig. 1) and its vibrational spectra (Table 1) calculations. The Hessian matrix in the ground singlet state (S<sub>0</sub>) and in the first excited triplet (T) state are used also for Franck-Condon factors estimations in absorption and emission spectra [10-13]. Infrared (IR) and Raman bands intensities are calculated by derivatives of dipole moment and of polarizability, respectively. Mulliken atomic charges in the ground S<sub>0</sub> state indicate that the Ru(II) ion is more close to the Ru(I) ion in the complex (0.726). Thus the polarization in the ligands can be analyzed from the DFT calculations. We use scaling factor 0.9756 for fitting

the calculated vibrational frequency to the available experimental data on 2,2'-bipyridine and bpy complexes with metals.

## 2. RESULTS AND DISCUSSION

Numeration of atoms of the optimized Ru(II)(bpy)<sub>2</sub>(CN)<sub>2</sub> complex structure is presented in Fig. 1. The Ru-N bonds, which are opposite to the CN ligands, have longer length (2.124 Å) than the Ru-N<sub>3</sub> (Ru-N<sub>16</sub>) bonds (2.076 Å) in agreement with the x-ray data (2.05 and 2.11 Å, respectively) [14]. The calculated C-C links in the ground S<sub>0</sub> state (1.474 Å) agree well with the x-ray data (1.481 Å); they are shortened to 1.425 Å in the T state. The bpy ligand bears the whole positive charge (0.118), while the CN ligand bears the whole negative charge (-0.481), the complex being electroneutral. Such polarization is quite convenient for interaction with TiO<sub>2</sub> surface.

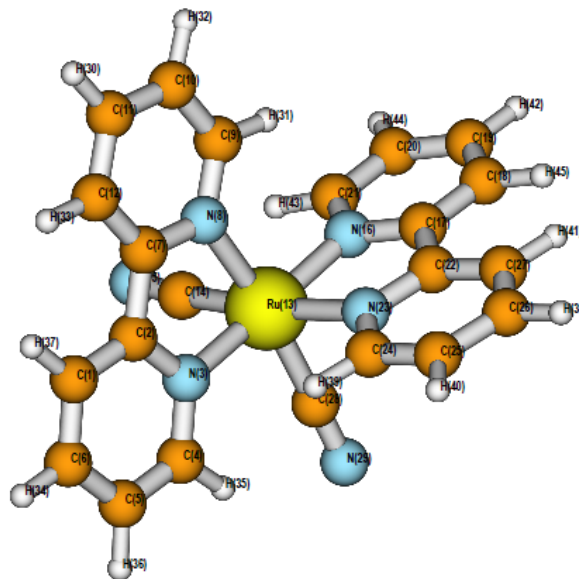


Figure 1. Optimized structure of [Ru(bpy)<sub>2</sub>(CN)<sub>2</sub>] complex.

Mode	Type of vibration	$\omega$	$I_{IR}$	$I_{Ram}$
113	$\nu(\text{CN})$ , in phase	2066	61.7	257.7
112	$\nu(\text{CN})$ , out-of-phase	2059	46.6	221.0
111	$\nu(\text{C}=\text{C})$ , $\nu(\text{C}-\text{C})$	1603	3.7	145.9
110	$\nu(\text{C}=\text{C})$ , $\nu(\text{C}-\text{C})$	1603	2.7	75.0
109	$\nu(\text{C}=\text{C})$ , $\nu(\text{C}-\text{C})$	1598	0.01	462.9
108	$\nu(\text{C}=\text{C})$ , $\nu(\text{C}-\text{C})$	1598	1.2	224.1
107	$\nu(\text{C}=\text{C})$ , $\nu(\text{C}=\text{N})$	1563	6.0	13.9
106	$\nu(\text{C}=\text{C})$ , $\nu(\text{C}=\text{N})$	1563	3.1	30.0

105	$\nu(\text{C}=\text{C}), \nu(\text{C}=\text{N})$	1550	0.1	179.0
104	$\nu(\text{C}=\text{C}), \nu(\text{C}=\text{N})$	1549	0.6	50.7
103	$\nu(\text{C}-\text{C}),$ in phase	1483	4.4	350.0
102	$\nu(\text{C}-\text{C}),$ out-of- phase	1479	62.3	122.9
101	$\delta(\text{CH})+\nu(\text{C}=\text{N})$ chel.	1463	36.9	13.7
100	$\delta(\text{CH})+\nu(\text{C}=\text{N})$ chel.	1460	113.2	1.1
99	$\delta(\text{CH})+\nu(\text{C}=\text{N})$ chel.	1436	5.9	21.8
98	$\delta(\text{CH})+\nu(\text{C}=\text{N})$ chel.	1435	5.6	14.3
97	$\delta(\text{CH})+\nu(\text{C}-\text{C})$	1423	68.1	5.9
96	$\delta(\text{CH})+\nu(\text{C}-\text{C})$	1422	11.9	16.1
95	$\nu(\text{C}=\text{N})$ chel.+ $\delta(\text{CH})$	1321	0.8	163.9
94	$\nu(\text{C}=\text{N})$ chel.+ $\delta(\text{CH})$	1321	2.1	86.2
93	$\nu(\text{C}-\text{C})+\delta(\text{CH})$	1321	4.1	24.9
92	$\nu(\text{C}-\text{C})+\delta(\text{CH})$	1320	2.1	298.4
91	$\nu(\text{C}=\text{N})+\nu(\text{C}=\text{C})+\delta(\angle\text{NRuN})$	1291	23.0	44.1
90	$\nu(\text{C}=\text{N})+\nu(\text{C}=\text{C})+\delta(\angle\text{NRuN})$	1289	4.7	68.8
89	$\nu(\text{C}=\text{N})+\nu(\text{C}=\text{C})+\delta(\text{CH})$	1277	3.1	76.6
88	$\nu(\text{C}=\text{N})+\nu(\text{C}=\text{C})+\delta(\text{CH})$	1275	26.3	51.4
87	$\nu(\text{C}=\text{N})+\nu(\text{C}=\text{C})+\delta(\text{CH})$	1273	4.8	126.2
86	$\nu(\text{C}=\text{N})+\nu(\text{C}=\text{C})+\delta(\text{CH})$	1272	9.7	30.6
85	$\delta(\text{CH})$	1182	0.1	50.9
84	$\delta(\text{CH})$	1182	0.1	18.4
83	$\delta(\text{CH})$	1173	3.7	1.1
82	$\delta(\text{CH})$	1173	2.0	4.1
79	$\delta(\text{CH})+\nu(\text{ring})$	1101	0.1	9.4
78	$\delta(\text{CH})+\nu(\text{ring})$	1100	0.1	3.8
75	$\delta(\text{CH})+\nu(\text{ring})$	1052	5.6	12.9
74	$\delta(\text{CH})+\nu(\text{ring})$	1052	1.3	73.6
73	$\delta(\text{ring})+\nu(\text{Ru}-\text{N})$	1036	1.7	2.6
72	$\delta(\text{ring})+\nu(\text{Ru}-\text{N})$	1034	2.6	0.7
69	ring breathing	1011	3.9	361.0
68	$\gamma(\text{CH})$	1001	0.7	1.93
67	$\gamma(\text{CH})$	1001	1.5	29.2
66	ring breathing	997	61.1	153.3
63	ring breathing	988	2.1	212.3
62	ring breathing	984	13.7	100.7
53	$\gamma(\text{CH})$	777	160.3	1.0
52	$\gamma(\text{CH})$	776	124.1	0.5
51	ring breathing	761	0.2	58.2
50	ring breathing	760	5.8	20.6
47	$\gamma(\text{CH})$	748	18.8	1.5
46	$\gamma(\text{CH})$	747	12.1	2.8
35	$\omega(\text{RuC})+$ ring twisting	484	4.9	0.7
34	$\tau(\text{RuC})+$ ring twisting	473	0.00	9.1
33	$r(\text{RuC})+\gamma(\text{ring})$	467	2.7	7.4
32	$\delta(b\angle\text{CRuC})+\gamma(\text{ring})$	464	1.2	5.6
31	$\nu(\text{Ru}-\text{C})$ in phase + $\gamma(\text{ring})$	454	0.5	13.3
30	$\nu(\text{Ru}-\text{C})$ out-of-phase+ $\gamma(\text{ring})$	435	7.9	2.4
29	$\omega(\text{RuC})+\gamma(\text{ring})$	431	6.3	1.1
28	$\tau(\text{RuC})+\gamma(\text{ring})$	430	5.4	0.7
27	$\tau(\text{RuC})$	411	0.1	9.2
26	$\nu(\text{Ru}-\text{C})$ out-of-phase	403	1.5	7.1
25	$\delta(b\angle\text{CRuC})+\gamma(\text{ring})$	383	7.8	3.2
24	$r(\text{RuC})+\gamma(\text{ring})$	376	9.3	0.9
23	$\nu(\text{Ru}-\text{C})$ in phase	360	0.1	17.7
22	$\nu(\text{Ru}-\text{N})$ out-of-phase	359	5.3	8.9

Table 1. IR and Raman spectra calculated by DFT method.

A number of the most interesting vibrational modes in the middle part of the IR and Raman spectra are presented in Table 1. Here  $\omega$  is a wavenumber ( $\text{cm}^{-1}$ ),  $I_{\text{IR}}$  is IR absorption intensity ( $\text{km/mol}$ ),  $I_{\text{Ram}}$  is the Raman scattering intensity ( $\text{\AA}^4/\text{amu}$ ). The valence C–H (stretching) vibrations (at about  $3200 \text{ cm}^{-1}$ ) are not shown in Fig. 2–3 and in Table 1, as well as the low-frequency modes ( $291\text{--}29 \text{ cm}^{-1}$ ).

## 2.1. IR spectrum

Valence vibrations of the C=C bonds with small admixture of the C–C links occur in the narrow region near  $1600 \text{ cm}^{-1}$  (111–108 modes, Table 1). They are very active in Raman scattering, but have low IR intensity. In the SERRS spectrum of the similar  $\text{Fe(II)(bpy)}_2(\text{CN})_2$  complex the 111 mode is found at  $1604 \text{ cm}^{-1}$  [15, 16] in a good fit with our result Table 1). Valence vibrations of the CN ligands at  $2066 \text{ cm}^{-1}$  are active in both IR and Raman spectra;  $\nu(\text{CN})$  modes of the in-phase and out-of-phase types are characteristic.

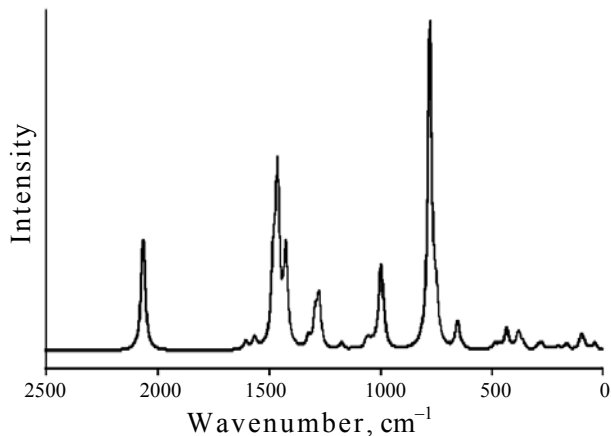


Figure 2. The calculated infrared spectrum of the  $[\text{Ru}(\text{bpy})_2(\text{CN})_2]$  complex.

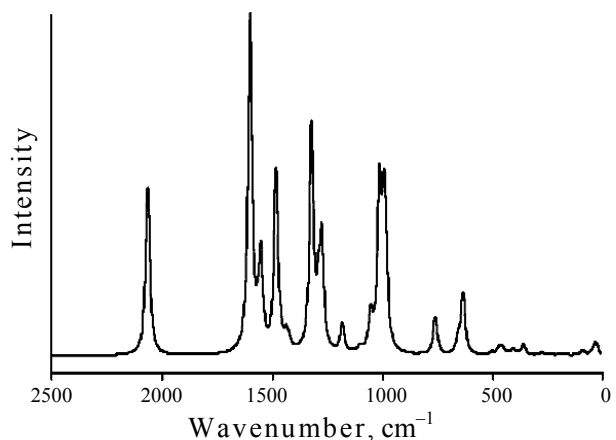


Figure 3. The calculated Raman spectrum of the  $[\text{Ru}(\text{bpy})_2(\text{CN})_2]$  complex.

They are more intense in Raman spectrum (Fig. 2–3). In a similar complex of Ir(III) ion this IR band has very low activity [3]. In the Table 1 the following notations are used:  $\nu$  – valence vibrations;  $\delta$  – deformation vibrations ( $\delta(b\angle)$  – scissoring);  $\gamma$  – out-of-plane vibrations;  $\tau$  – twisting vibrations;  $r$  – rocking vibrations;  $\omega$  – wagging vibrations.

Valence vibrations of the C–C links (102, 103 modes) are very important in respect to electron transfer upon light absorption [3], though they have not gain much attention from experimentalists [12–21]. They provide narrow IR band at about  $1480\text{ cm}^{-1}$  (Table 1, Fig. 2). The intense out-of-phase mode 102 gives a peak which is overlapped by a band of CH deformation vibrations (modes 101, 102). Ring breathing at  $997\text{ cm}^{-1}$  gives a narrow IR band of a middle intensity (mode 66); in Raman spectrum there are three close lying lines (modes 66–62) in the same region (Table 1, Fig. 3).

The most intense IR band occurs at  $777\text{ cm}^{-1}$  (modes 53, 52, Fig. 2 and 3, which are non active in Raman). This is out-of-plane CH vibration ( $\gamma(\text{CH})$ , Table 1). Vibration modes 35–24 in the range  $490$ – $370$  are assigned to stretching and deformation of Ru–C and Ru–N bonds. A great advantage of quantum chemical methods is that they can predict the low frequency vibrations, which are important in metal-to-ligand charge transfer process. The mode 30 ( $435\text{ cm}^{-1}$ ) is active in IR spectrum; it corresponds to out-of-phase Ru–C stretching in two CN ligands with simultaneous inter-ring bend ( $\gamma(\text{ring})$ ). Such interpretation,  $\gamma(\text{ring})$ , has been tentatively proposed for  $\text{Pd}(\text{bpy})\text{Cl}_2$  complex [19] for the weak IR band at  $448\text{ cm}^{-1}$ ; in our case this mode is mixed with the Ru–CN stretching. The Ru–N vibration (modes 22, 23) are rather weak to be fixed in IR absorption (Fig. 2, Table 1), but they have been observed in Raman scattering for similar complexes [12, 18, 19].

## 2.2. Raman spectrum

The Ru–N out-of-phase vibration (mode 22) gives the first weak band in Fig. 2; it is almost degenerate with the in-phase counterpart (Table 1). These two modes have been assigned to the band  $371\text{ cm}^{-1}$  in the SERRS spectrum of the  $[\text{Ru}(\text{bpy})_3]^{2+}$  complex [12]. Our DFT calculation reveals that these modes include pulsation of chelate cycles. In Raman spectrum of  $\text{Fe}(\text{bpy})_2(\text{CN})_2$  complex the bands at  $385$  and  $367\text{ cm}^{-1}$  have been assigned to Ru–N stretchings [12]. Such a large splitting between these two modes is non reliable; from our calculation we can assign the former band  $385\text{ cm}^{-1}$  to the out-of-phase stretching and deformations of Ru–C bonds (modes 25–27), but not to Ru–N by no means (Table 1).

Interaction of bipyridyl complexes with Ag sol provides a well-known surface-enhanced resonance Raman scattering (SERRS) [12]. The combination of resonance and surface enhancement in SERRS can lead to twelve orders of magnitude combined enhancement and to high sensitivity for micromolar concentrations. The enhancement is due to surface plasmon resonance, which

also leads to quenching of fluorescence and is connected with interface electron transfer. Since the SERRS is important for probing the dye-metal surface interaction at low concentrations, it is useful to know complete assignment of Raman spectra of the dye-sensitizer in order to improve the IPCCE value for solar cells. Comparison of theoretical IR and Raman spectra (Fig. 2 and 3, Table 1) is very useful in this respect.

In solar cells the dye interacts with nanocrystalline semiconductor surface by CN ligands. Stretching vibrations of the CN ligands split into  $2066$  and  $2059\text{ cm}^{-1}$  (in-phase and out-of-phase) are very active in Raman spectrum (Table 1). One can expect that they would be enhanced upon the dye-surface interaction and participate in electron-transfer process responsible for IPCCE parameter of the solar cell.

The most intense Raman band at  $1598\text{ cm}^{-1}$  (modes 111–108) is determined by C=C stretching vibrations of the bpy rings with small contributions of the C–C links. In the SERRS spectra of the  $\text{Fe}(\text{bpy})_2(\text{CN})_2$  dye the C=C band is observed at  $1604\text{ cm}^{-1}$  [12]. Similar bands are detected for a number of bpy complexes [16].

Interaction of C=C and C=N vibrations of the bpy cycles leads to Raman bands at  $1563$ – $1550\text{ cm}^{-1}$  of middle intensity (modes 107–104, Table 1). Such bands have been observed in the resonance Raman scattering of the  $\text{Fe}(\text{bpy})_2(\text{CN})_2$  and the  $[\text{Ru}(\text{bpy})_3]^{2+}$  complexes at  $1564$  and  $1562\text{ cm}^{-1}$ , respectively, and assigned to C=C stretchings [12]. This is not exactly the same assignment what we get in our calculation.

Our DFT calculation indicates that vibrations of the C–C inter-rings link are very intense in Raman spectrum (modes 102, 103, Table 1), especially in the triplet excited state. The main intense band in this region ( $1483\text{ cm}^{-1}$ , Table 1) has been observed at  $1489\text{ cm}^{-1}$  and assigned to the mixed vibrations,  $\nu(\text{C–C})+\delta(\text{CH})$ , [12] in the SERRS spectrum of  $\text{Fe}(\text{bpy})_2(\text{CN})_2$  complex. We get other assignments (Table 1), which agrees with ref. [10, 11]; the late modes are calculated at  $1320\text{ cm}^{-1}$  (the 93, 92 modes). An intense peak in the SERRS spectrum of  $\text{Ru}(\text{bpy})_2(\text{BIK})^{2+}$  complex (BIK is bis(1-methylimidazol-2-yl)ketone) is found at  $1317\text{ cm}^{-1}$  [11] and can be assigned to the C–C inter-rings stretching vibration mixed with the  $\delta(\text{CH})$  deformations. In the close region we get also a number of mixed vibrations (modes 91–87) which are quite active in Raman spectrum (Table 1, Fig. 3). These are mostly the C=N vibrations in bpy rings mixed with C=C stretching and  $\delta(\text{CH})$  deformations. Strukl and Walter [19] assigned a weak IR band at  $1265$ – $1280\text{ cm}^{-1}$  in  $\text{M}(\text{bpy})\text{Cl}_2$  complexes to the C–C inter-rings vibration and now we can decline such assignment.

## CONCLUSIONS

We can not find direct experimental data on IR and Raman spectra of the studied complex, but the measurements for similar systems are available. Our DFT

calculations with a scaling factor (0.9756) obtained by fitting the calculated vibration frequency to the available experimental data on 2,2'-bipyridine provide quite reasonable agreement for some similar bpy complexes with different metals. Thus we hope that our calculation for the Ru(bpy)<sub>2</sub>(CN)<sub>2</sub> complex provides quite reasonable prediction for its IR and Raman spectra. We have changed some assignments published in the literature [12, 15–21] for IR, Raman and SERRS spectra of the [Ru(bpy)<sub>3</sub>]<sup>2+</sup>, Ru(bpy)<sub>2</sub>(bis(1-methylimidazol-2-yl)ketone)<sup>2+</sup> and Fe(bpy)<sub>2</sub>(CN)<sub>2</sub> complexes. The simple Ru(II)(bpy)<sub>2</sub>(CN)<sub>2</sub> complex studied in the present work by DFT method with optimized structure and vibrational analysis can be used as a model species for dye-sensitized solar cells in order to predict the role of vibronic perturbations in absorption spectra and interface electron transfer rate.

## REFERENCES

- [1] A. Hagfeldt, M. Gratzel, *Acc. Chem. Res.* 33, 269, 2000.
- [2] J. E. Monat, J. H. Rodriguez, J. K. McCusker, *J. Phys. Chem. A*, 106, 7399, 2002.
- [3] B. Minaev, V. Minaeva, O. Vahtras, *Proceedings of the Nano-Sol-Net International Symposium: Trends in Organic Electronics and Hybrid Photovoltaic's*, edited by M.A. Girtu and M. Fahlman, Eforie Nord, Romania, June 12–14, 2008. Constanta, Ovidius Univ. Press, 48, 2008.
- [4] F. Aiga, T. Tada, *J. Mol. Struct.* 658, 25, 2003.
- [5] B. Minaev, V. Minaeva, H. Agren, *J. Phys. Chem. A*, 113, 726, 2009.
- [6] A. D. Becke, *J. Chem. Phys.* 98, 5648, 1993.
- [7] K. Burke, J. Werschnik, E. K. U. Gross, *J. Chem. Phys.* 123, 062206, 2005.
- [8] C. Lee, W. Yang, R. G. Parr, *Phys. Rev.* 37, 785, 1988.
- [9] M. J. Frisch, G. W. Trucks, H. B. Schlegel, G. E. Scuseria, M. A. Robb, J. R. Cheeseman, J. A. Montgomery, Jr., T. Vreven, K. N. Kudin, J. C. Burant, J. M. Millam, S. S. Iyengar, J. Tomasi, V. Barone, B. Mennucci, M. Cossi, G. Scalmani, N. Rega, G. A. Petersson, H. Nakatsuji, M. Hada, M. Ehara, K. Toyota, R. Fukuda, J. Hasegawa, M. Ishida, T. Nakajima, Y. Honda, O. Kitao, H. Nakai, M. Klene, X. Li, J. E. Knox, H. P. Hratchian, J. B. Cross, C. Adamo, J. Jaramillo, R. Gomperts, R. E. Stratmann, O. Yazyev, A. J. Austin, R. Cammi, C. Pomelli, J. W. Ochterski, P. Y. Ayala, K. Morokuma, G. A. Voth, P. Salvador, J. J. Dannenberg, V. G. Zakrzewski, S. Dapprich, A. D. Daniels, M. C. Strain, O. Farkas, D. K. Malick, A. D. Rabuck, K. Raghavachari, J. B. Foresman, J. V. Ortiz, Q. Cui, A. G. Baboul, S. Clifford, J. Cioslowski, B. B. Stefanov, G. Liu, A. Liashenko, P. Piskorz, I. Komaromi, R. L. Martin, D. J. Fox, T. Keith, M. A. Al-Laham, C. Y. Peng, A. Nanayakkara, M. Challacombe, P. M. W. Gill, B. Johnson, W. Chen, M. W. Wong, C. Gonzalez, and J. A. Pople, *Gaussian 03*, revision C.02, Gaussian, Inc., Wallingford, CT, 2004.
- [10] Y. M. Jang, S. Nam, J. W. Lim, H. J. Yeo, M. S. Lee, *Bull. Korean Chem. Soc.* 19, 372, 1998.
- [11] Y. M. Jang, J. W. Lim, E. R. Kim, H. Lee, M. S. Lee, *Bull. Korean Chem. Soc.* 22, 318, 2001.
- [12] T. J. Dines, R. D. Peacock, *J. Chem. Soc. Faraday Trans. 1*, 84, 3445, 1988.
- [13] L. J. Bellamy *The infrared spectra of Complex molecules*. London: Chapman & Hall, 1, 1975, 433 p.
- [14] J.-F. Guillemoles, V. Barone, L. Joubert, C. Adamo, *J. Phys. Chem. A*, 106, 11354, 2002.
- [15] T. A. Heimer, C. A. Bignozzi, G. J. Meyer, *J. Phys. Chem.* 97, 11987, 1993.
- [16] M. Muniz-Miranda, *J. Raman Spectrosc.* 31, 637, 2000.
- [17] E. Gastellucci, L. Angeloni, N. Neto, G. Sbrana, *Chem. Phys.* 43, 365, 1979.
- [18] J. S. Strukl, J. L. Walter, *Spectrochimica Acta*, 27A, 209, 1971.
- [19] J. S. Strukl, J. L. Walter, *Spectrochimica Acta*, 27A, 223, 1971.
- [20] P. Matejka, J. Stavek, K. Volka, B. Schrader, *Applied Spectroscopy*, 50, 409, 1996.
- [21] I. Srnova, B. Vlekova, V. Baumruk, *J. of Molecular Structure*, 410–411, 201, 1997.